RESONANCES FOR INTERMITTENT SYSTEMS

V. Baladi and J.-P. Eckmann
Section de Mathématiques
Université de Genève
CH-1211 Geneva 4, Switzerland

D. Ruelle
I.H.E.S., 91440 Bures-sur-Yvette, France

RESONANCES FOR INTERMITTENT SYSTEMS

V. Baladi and J.-P. Eckmann

Section de Mathématiques
Université de Genève
CH-1211 Geneva 4, Switzerland

D. Ruelle

IHES
F-91440 Bures-sur-Yvette, France

Abstract. There is increasing theoretical and numerical evidence that for many interesting dynamical systems the power spectrum of an observable A extends to a meromorphic function in the complex frequency plane. The position of the complex poles or "resonances" is independent of the observable A which is monitored. In this paper, we study the resonances for intermittent dynamical systems by using a probabilistic independence assumption about recurrence times. A close agreement between theory and numerical experiments is obtained.

1. Introduction

It has been known for some time [10] that dynamical systems may have time correlation functions which decay "abnormally", even when they are very chaotic. As an example, there are mixing Axiom-A flows, for which the time correlation functions do not decay exponentially.* In the case of mixing Axiom-A diffeomorphisms, the decay rate is always exponential, but the correlation function itself may be strongly modulated, see Fig. 1.
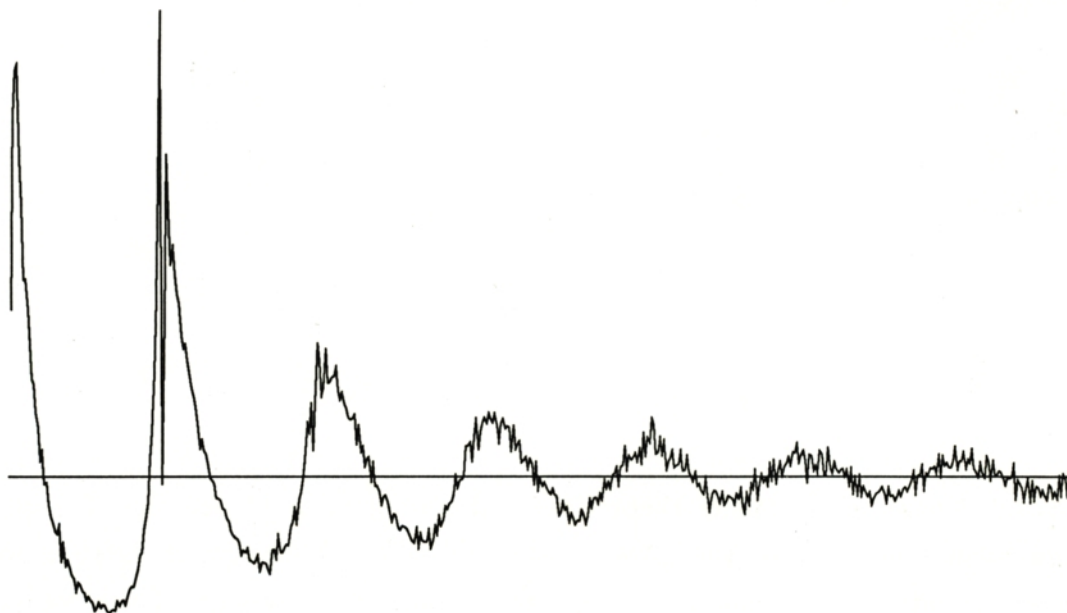

Fig. 1: The time correlation function C_k for the map f_ϵ of Eq.(3.1) with $\epsilon = 0.001$, for $k = 0, \ldots, 512$.

An adequate description of these modulations can be obtained by considering the Fourier transform $\hat{C}(\omega)$ of the correlation function C_k. $\hat{C}(\omega)$ is called the power spectrum. Clearly, if, for example, $C_k = \exp(-\lambda|k|)\cos(\alpha|k|)$, then $\hat{C}(\omega)$ has complex poles at $\omega = \pm\alpha \pm i\lambda$. Such poles have been studied in a sequence of papers [11, 12, 8], in which it was shown that for Axiom-A diffeomorphisms, the Fourier transform of $C(t)$ is meromorphic in a region $|\text{Im}\,\omega| < \alpha_0$, i.e., the singularities in this region can at worst be poles. If the poles stay at a finite distance from the real axis, the correlation function

---

* So far, however, no example of this phenomenon with an Axiom-A attractor is known.

decays exponentially, and it is modulated if the poles are not purely imaginary. If the poles come arbitrarily close to the real axis (which is possible in the case of Axiom-A flows [10]), then the decay will not be exponential.

In this paper we discuss a dynamical mechanism which is responsible for the modulations of the correlation functions and predicts them in terms of orbits. This mechanism occurs in systems for which one can define consecutive time intervals ("laps") with approximately independent behavior. *The positions of the complex poles of the power spectrum – also called resonances – are given in terms of the probabilistic distribution* Δ *of the duration of these laps.* If Δ is Gaussian, very simple scaling relations are obtained.

This formalism is especially suited for discrete time dynamical systems with Type I intermittency in the sense of Pomeau and Manneville [9] (this is intermittency caused by the "collision" of a stable and an unstable periodic orbit, as a parameter is varied, i.e., by a saddle-node bifurcation, cf. Fig. 1). The laps are separated by the end of a laminar period. We show how Δ can be calculated from a few dynamical parameters, which therefore suffice to predict the poles of the correlation function. There will be *two* basic modulation frequencies associated with an intermittent orbit: The first (fast) frequency is the period onto which one almost locks, and the second (slow) frequency is given through the mean return time. Thus, *modulated correlation functions occur for intermittent systems.* Of course, in a complicated dynamical system, a number of different periodic orbits may be visited intermittently by the physical orbit; in that case, the signal will be a superposition of several of the simple phenomena we are describing and may be hard to disentangle.

The present work is closely related to papers by Mori *et al.* [6, 7] which are also concerned with the question of modulated correlation functions. Our discussion is, however, centered on *complex* poles in frequency space and their relation with the distribution Δ, whereas in [6, 7] the authors consider in particular the typical shapes of the real power spectrum for various types of intermittency.

One may ask what relevance the results of the present papers have for the rigorous study of differentiable dynamical systems. Since our results depend on the assumption of statistical independence of successive laps, they cannot give any proof of analyticity for the power spectrum. On the other hand, they give a strong indication of the presence

of certain singularities and how close these are to the real axis. Consider for instance the maps $x \mapsto ax(1-x)$ of the interval $[0,1]$; since saddle-node bifurcations and intermittency occur frequently in the chaotic parameter region, we expect that arbitrarily slow mixing rate will also occur frequently.

In Section 2, we describe the general mechanism of how an intermittent recurrence can lead to poles in the Fourier transform of C_k. We apply this method in Section 3 for the case of intermittency of Type I. We describe how the pole(s) move in the complex plane as a function of the bifurcation parameter and compare our theoretical predictions with numerical experiments. Finally, in Section 4, we illustrate these ideas on a saddle-node bifurcation from a period 3.

2. A Model for Correlation Functions of Intermittent Dynamical Systems

We consider a dynamical system with continuous time* and we denote by $f^t x = x_t$ the phase point reached after time t, if at time 0 we were at x. We also denote by A and B some observables, i.e., functions from phase space to $\mathbf{R}$ (or, more generally $\mathbf{R}^N$), and by $\langle F \rangle$ the ergodic average

$$\langle F \rangle = \lim_{T \to \infty} \frac{1}{T} \int_0^T d\tau F(f^\tau x) \ .$$

The correlation function is then defined by

$$\begin{aligned}
\rho_{AB}(t) &= \lim_{T \to \infty} \frac{1}{T} \int_0^T d\tau \, A(f^\tau x) \, B(f^{\tau+t}x) - \langle A \rangle \langle B \rangle \\
&= \langle A \, (B \circ f^t) \rangle - \langle A \rangle \langle B \rangle \ .
\end{aligned} \tag{2.1}$$

To simplify matters we will suppose that $\langle A \rangle$ and $\langle B \rangle$ vanish.

We now make the main working assumption:

---

* For simplicity, we shall use interchangeably discrete and continuous time systems.

A) *There is a sequence of times* $t_1 < \ldots < t_n < \ldots$ *such that*

 a) *The differences* $t_n - t_{n-1}$ *form a sequence of independent, identically distributed random variables (with distribution* $\Delta(t)dt$ *).*

 b) *The orbit before and after* t_n *is distributed independently of* n. *More precisely, the functions* $t \mapsto x_{t_{n-1}+t}$ *defined on* $[0, t_n - t_{n-1}]$ *are independent, identically distributed objects.**

A sequence of x_t satisfying Assumption A is also known as a regenerative process. We define $I_n = [t_{n-1}, t_n]$. Let us hasten to explain the meaning of this construction – an even more concrete determination of the I_n will be given in the next section. A typical way to define the time intervals I_n is to say that they *end* at the time when something "special" happens in phase space. E.g., I_n may end when the orbit leaves a given region of phase space; in the case of intermittency this will be the end of the "laminar" period (defined in some arbitrary way). When I_n ends, I_{n+1} starts.

Assumption A of course contradicts the determinism of the time evolution, but one should note that the assumption is a reasonable approximation for what happens for "intermittent" systems in which chaotic behavior alternates with laminar intervals. Namely, the length of one laminar interval is in some sense independent of how long the preceding laminar interval was. In the same way, the times spent on each side of the Lorenz attractor [5] are well approximated by a probability distribution of independent random variables.

By Assumption A, the length t of the time interval I_n is a random variable; we denote by $\Delta(t)$ its probability density. We next relate Δ to the poles of the Fourier transform $\hat{\rho}_{AB}$ of ρ_{AB}. If we let $\rho_{AB}^+(t) = \rho_{AB}(t)\theta(t)$, with

$$\theta(t) = \begin{cases} 1 & \text{if } t \geq 0 \\ 0 & \text{if } t < 0, \end{cases}$$

and $\rho_{AB}^-(t) = \rho_{AB}^+(-t)$, we have

$$\rho_{AB}(t) = \rho_{AB}^+(t) + \rho_{BA}^+(-t) = \rho_{AB}^+(t) + \rho_{BA}^-(t) ,$$

---

* In particular, if the length $t_n - t_{n-1}$ of the interval is fixed and $t \in [0, t_n - t_{n-1}]$, then $x_{t_{n-1}+t}$ has a distribution $\bar{\Delta}_{t_n - t_{n-1}, t}(x)dx$.

so that it will suffice to study ρ_{AB}^+. We may write

$$\rho_{AB}^+(t_2 - t_1) = \sum_{m=0}^{\infty} \rho_{AB,m}^+(t_2 - t_1) \,,$$

where $\rho_{AB,m}^+$ is the correlation ρ_{AB}^+ conditioned by "if $t_1 \in I_n$ then $t_2 \in I_{m+n}$". Given Assumption A it will be quite easy to compute $\rho_{AB,m}^+$. We denote by $P_A(X,u)$ the probability density that $A(f^t x) = X$ and that the interval I_n in which t lies is being exited at time $t+u$. This probability does not depend on n by Assumption A. Similarly, $Q_B(Y,v)$ denotes the probability density that $B(f^t x) = Y$ and that the interval I_n in which t lies was entered at time $t - v$. For $m \geq 1$, the orbit has to "traverse" $m - 1$ intervals, and this leads to

$$\begin{aligned}
\rho_{AB,m}^+ &= \int_0^{\infty} du \int_0^{\infty} dv \, \Delta^{*(m-1)}(t - u - v) \\
&\quad \times \int dX \, X P_A(X,u) \int dY \, Y Q_B(Y,v) \\
&= (F_A * G_B * \Delta^{*(m-1)})(t) \,,
\end{aligned} \tag{2.2}$$

where

$$\begin{aligned}
F_A(s) &= \int dX \, X P_A(X,s) \,, \\
G_B(s) &= \int dY \, Y Q_B(Y,s) \,,
\end{aligned}$$

and where we denote by Δ^{*k} the k-fold convolution product $\Delta * \cdots * \Delta$ (and $\Delta^{*0}(t) = \delta(t)$). Finally, if $m = 0$, we have

$$\rho_{AB,0}^+(t_2 - t_1) \leq \max_x |A(x)| \max_y |B(y)| \times \mathrm{Prob}\{t_1 \text{ and } t_2 \text{ lie in the same } I_n\}.$$

To proceed, we assume that

$$\Delta(t) \leq \mathrm{const.} e^{-\lambda t} \,, \tag{2.3}$$

with $\lambda > 0$. Then $\rho_{AB,0}^+$, F_A, and G_B also decay exponentially. By construction, they vanish for negative arguments. It follows that their Fourier transforms, $\hat{\rho}_{AB,0}^+$, $\hat{F}_A$, and $\hat{G}_B$ extend holomorphically to $\mathrm{Im}\,\omega < \lambda$, (we have written $\hat{f}(\omega) = \int dt \, e^{-i\omega t} f(t)$), and

$$\hat{\rho}_{AB}^+(\omega) = \sum_{m=0}^{\infty} \hat{\rho}_{AB,m}^+(\omega) = \hat{\rho}_{AB,0}^+(\omega) + \frac{\hat{F}_A(\omega)\hat{G}_B(\omega)}{1 - \hat{\Delta}(\omega)} \,.$$

Therefore, $\hat{\rho}_{AB}^{+}$ is meromorphic for $\mathrm{Im}\,\omega < \lambda$ and holomorphic for $\mathrm{Im}\,\omega < 0$. Similarly, $\hat{\rho}_{BA}^{-}(\omega)$ is meromorphic for $\mathrm{Im}\,\omega > -\lambda$, and holomorphic for $\mathrm{Im}\,\omega > 0$. Thus, we have shown

Lemma 2.1. *Under the Assumption A, and if (2.3) holds, $\hat{\rho}_{AB}(\omega)$ is meromorphic for $|\mathrm{Im}\,\omega| < \lambda$ and its poles in $\mathrm{Im}\,\omega > 0$ are those of $\hat{\rho}_{AB}^{+}(\omega)$ and are roots of*

$$1 = \hat{\Delta}(\omega) . \tag{2.4}$$

It is instructive to consider the case of a Gaussian distribution $\Delta(t)$, although this gives a non-zero probability for negative times. If we assume that Δ is Gaussian, with mean T and variance σ^2, then its Fourier transform is

$$\hat{\Delta}(\omega) = e^{-\sigma^2 \omega^2 / 2}\, e^{-i\omega T} .$$

Therefore, $\hat{\Delta}(\omega) = 1$ means

$$\frac{\sigma^2}{2}\omega^2 + iT\omega - 2\pi i k = 0 ,$$

and this has the solutions

$$\omega = \frac{T}{\sigma^2}\left(-i \pm \sqrt{-1 + \frac{4\pi i k \sigma^2}{T^2}}\right) .$$

We are mainly interested in the roots which are close to the real axis. If $\sigma^2/T^2 \ll 1$, then we can expand the above solutions. We find that the poles of the correlation function near zero with positive imaginary part are located at

$$
\begin{aligned}
\omega_k &= \frac{iT}{\sigma^2}\left(-1 + \sqrt{1 - \frac{4\pi i k \sigma^2}{T^2}}\right) \\
&= \frac{iT}{\sigma^2}\left(-\frac{2\pi i k \sigma^2}{T^2} - \frac{2\pi^2 i^2 k^2 \sigma^4}{T^4} + \mathcal{O}\big((k\sigma^2/T^2)^3\big)\right) \\
&= \frac{2\pi k}{T} + i\frac{2\pi^2 k^2 \sigma^2}{T^3} + \mathcal{O}\big(k^3 \sigma^4/T^5\big) .
\end{aligned}
\tag{2.5}
$$

Note that, to leading order, the real part of the resonance does not depend on σ^2, and that the imaginary part, i.e., the decay rate of the correlation function, is of order

σ^2/T^3. Thus, *the correlation function is modulated with period T, and decays at a rate* $2\pi^2\sigma^2 T^{-3}$.

Remark. The division of the time axis into the I_n is arbitrary, but the resulting poles are independent of this division. E.g., if we lump together 2 consecutive intervals to make a new one, then (2.4) is replaced by

$$1 = \hat{\Delta}(\omega)^2 ,$$

which has the same roots as (2.4) (and some additional roots with residue 0).

3. An Intermittent Fixed Point

We consider in detail a specific example and calculate explicitly several of the relevant quantities which we then compare with numerical experiments. We work with the one-parameter family of maps $f_\epsilon : [-1,1] \to [-1,1]$ defined by

$$f_\epsilon(x) = \begin{cases} g_\epsilon(x), & \text{if } |g_\epsilon(x)| \le 1 \\ g_\epsilon(x) - 2, & \text{if } |g_\epsilon(x)| > 1 \end{cases} \tag{3.1}$$

and

$$g_\epsilon(x) = x + \kappa x^2 + \epsilon, \quad \kappa = 1.75 .$$

We view f_ϵ as a discrete time dynamical system. For $\epsilon = 0$ the graph of f_ϵ is illustrated in Fig. 2.

We derive now an expression for Δ by analyzing f_ϵ. This will lead to an expression for C_k which we work out in part. Along the way, we check the validity of several working assumptions by comparing them with numerical experiments. When ϵ is positive (but small), the fixed point at zero disappears (into the complex) and the iterated map f_ϵ leads to a very slow motion near $x = 0$. It is well known that this motion can be accurately described in terms of a differential equation [9]: From

$$x_{n+1} - x_n = \kappa x_n^2 + \epsilon , \tag{3.2}$$

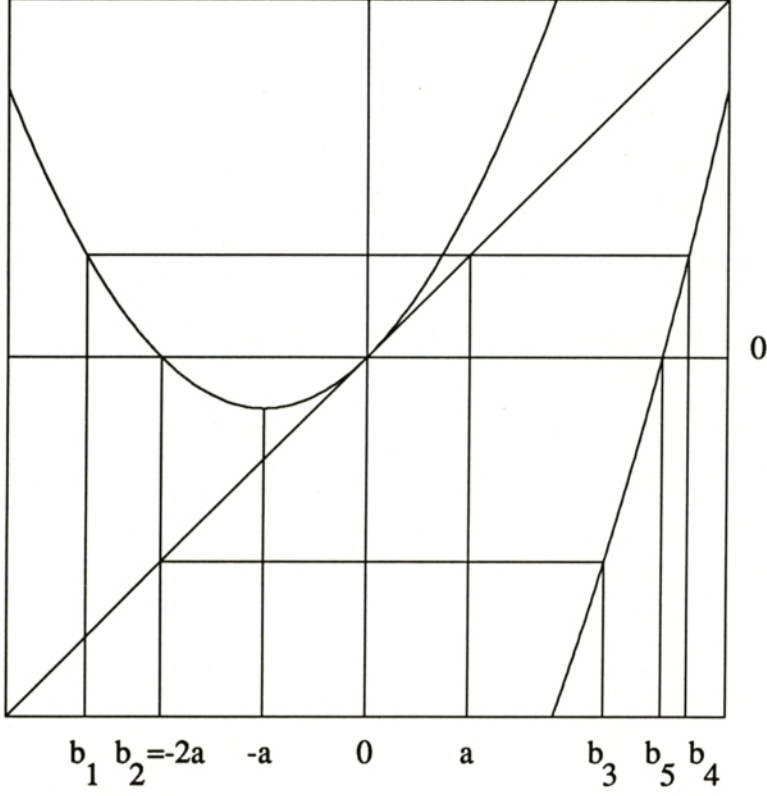we conclude that

$$\frac{dx}{dn} = \kappa x_n^2 + \epsilon ,$$

Fig. 2: Graph of f_ϵ and the various intervals discussed in the paper.

or

$$\frac{dn}{dx} = \frac{1}{\kappa x_n^2 + \epsilon} \cdot$$

Integrating, we find

$$n(x) = n_0 + \frac{1}{(\epsilon\kappa)^{1/2}} \arctan\big((\kappa/\epsilon)^{1/2}x\big) \tag{3.3}$$

and finally

$$x_n = \left(\frac{\epsilon}{\kappa}\right)^{1/2} \tan\big((\epsilon\kappa)^{1/2}(n - n_0)\big) . \tag{3.4}$$

Equation(3.4) is a good approximation as long as $x_{n+1} - x_n$ is small, which is true as long as $(\kappa x_n^2 + \epsilon)^{-1} \gg 1$. To get simpler expressions, we shall use (3.4) even for the few time steps where the above inequality does not hold. (In the limit when ϵ tends to 0, this results in errors which are seen to be negligible with respect to the leading order.)

We define, somewhat arbitrarily, the intervals I_n by the exits from the "laminar" region $x \in [-4/7, 2/7]$. More precisely, the time interval I_n begins one time step after I_{n-1} ends; we call t_n the entry time of I_n. The motion is then called non-laminar until the orbit enters the interval $[-a', a]$, where $a = 2/7$ and $-a' = -4/7$.[*] Thereafter, the orbit is called laminar, and I_n ends when the orbit is laminar and is about to cross the boundary of $[-a', a]$ at $a = 2/7$. We shall say that the orbit is reinjected into $[-a', a]$ at time r_n, cf. Fig. 2. These concepts are similar to those described in [1].

We analyze this situation in the case of very small, but positive, ϵ in which we again neglect higher order terms. Note that the time needed to cross the interval $[-a', a]$ is of order $\mathcal{O}(\epsilon^{-1/2})$, which grows without bounds as $\epsilon \to 0$, while the time of non-laminarity, i.e., the time between entering I_n and entering $[-a', a]$ grows more slowly, and is on average bounded, by $\mathcal{O}(1)$, see below. The time interval $[t_n, t_{n+1})$ can be viewed as a sum of two pieces, $[t_n, r_n)$, and $[r_n, t_{n+1})$. We now analyze these time intervals, the first being the "chaotic phase" and the second being the "laminar phase".

The first time interval is the time of chaotic behavior. We denote by $G(s)$ the probability that this interval has length equal to s. Our probabilistic assumptions say that $G(s)$ does not depend on the position at which the chaotic phase started. We want to argue that for large s,

$$G(s) = \mathcal{O}((1-p)^s) , \tag{3.5}$$

where p is a "dying probability" which we model now. In the absence of special resonances, and we will assume this henceforth, the following happens. The orbit starts at some point to the right of $a = 2/7$ and is then governed by the action of the *expanding* map $f_\epsilon|_{[-1,1]\setminus[-a',a]}$, until it is reinjected into $[-a', a]$. Therefore, with good approximation, we may assume that there is a corresponding absolutely continuous invariant measure, so that the reinjection takes place with probability p per unit of time.[**] Note that because of the deterministic nature of the map, the first return to $[-a', a]$ cannot take place before the point has moved from a to the rightmost branch of the graph of f_ϵ, and therefore $G(s)$ does *not* start out to be a power law like in (3.5). The discrete conditions one encounters for small s make it hard to give a general theory for G for small s. In any case, we expect G to be zero for small s and behave then like a decaying

---

[*] Note that $\partial_x f_\epsilon(-a) = 0$ and when $\epsilon = 0$, then $f_\epsilon(-a') = 0$.

[**] If we further assume that the invariant measure is constant, then p is given as the quotient u/v, where v is the length of the intervals $[-1, 1] \setminus [-a', a]$, and u is the length of the preimage of $[-a', a]$ in $[-1, 1] \setminus [-a', a]$. This quotient is readily computed in our concrete case, cf. (3.1), we find $p \approx 0.385$.

exponential function. An experimental distribution of return times is shown in Fig. 3, together with an exponential fit of the form of (3.5) (with $p = 0.385$).
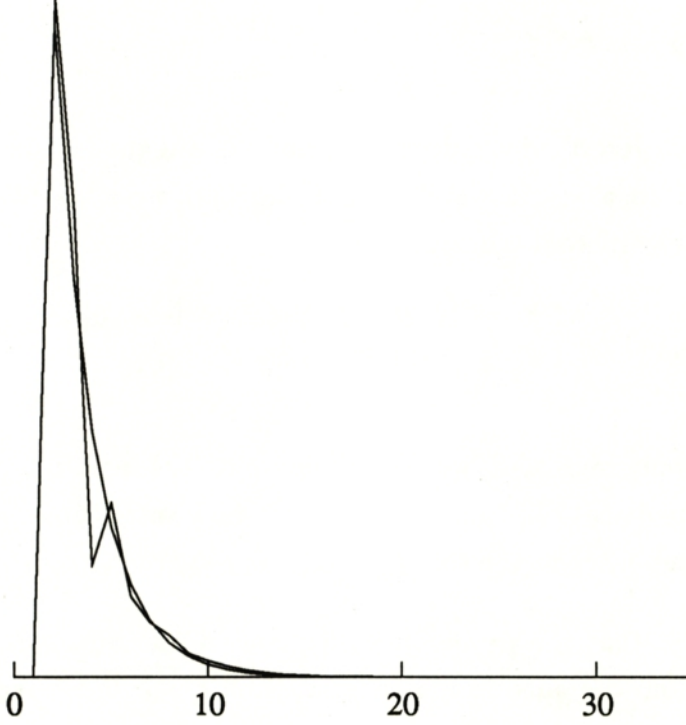

Fig. 3: The distribution of return times for $\epsilon = 0.012$, and theoretical prediction.

Now that we have a handle over the reinjection time, i.e., over the duration of the chaotic phase, we analyze the duration of the laminar phase. During the laminar phase the motion is simply a monotone increase of x_n in the interval $[-a', a]$ as n increases. The duration of the laminar motion depends only on the reinjection point in $[-a', a]$. Thus, in order estimate the distribution Δ, we have to study the distribution of this reinjection point. This reinjection density is induced by the distribution μ of the points in $[-1,1] \setminus [-a', a]$. The probability $h_1(x)dx$ to be injected into $[x, x + dx] \subset [-a', a]$ is then

$$h_1(x)dx = \sum_{y: f_\epsilon(y)=x} \mu(y)\frac{dx}{|f'_\epsilon(y)|} \cdot \qquad (3.6)$$

To find h_1, we consider the five points $b_1, \ldots, b_5$ defined as follows (cf. Fig. 2): b_1 is the negative preimage of a, and $b_2 = -a'$. Denote by b_4 the largest preimage of a and by b_3 the positive preimage of a'. Finally, b_5 is the zero of f_ϵ which lies between b_3 and

b_4. Using (3.6) and assuming for simplicity that $\mu(dx)$ is proportional to the Lebesgue measure dx, and that f'_ϵ is constant over the intervals $[b_1, b_2]$ and $[b_3, b_4]$, we estimate the probability $h_1(x)dx$ to land in the interval $[x, x + dx]$ as

$$h_1(x) = \begin{cases} \frac{1}{a'}\frac{2(b_4-b_3)}{3(b_4-b_3+b_2-b_1)}\,, & \text{when } x \in [-a', 0], \\ \frac{1}{a}\frac{3(b_2-b_1)+(b_4-b_3)}{3(b_4-b_3+b_2-b_1)}\,, & \text{when } x \in [0, a]. \end{cases}$$

The model we have just described is correct in principle, but the various approximations and assumptions lead to a result which is not the best possible fit.* We therefore continue with a slightly different Ansatz for h_1:

$$h_1(x) = \begin{cases} h_L \equiv 1/(2a'), & \text{when } x \in [-a', 0]\,, \\ h_R \equiv 1/(2a), & \text{when } x \in [0, a]\,. \end{cases} \tag{3.7}$$

Since (3.4) holds only in $[-a, a]$, we need to compute the injection density in $[-a, a]$ which is induced by the density h_1 in $[-a', a]$. This is easy since those points which land in $[-a', -a]$ are one step later in the set $[f_\epsilon(-a), 0] = [-1/7 + \epsilon, 0]$, which is in $[-a, a]$.

Using (3.6), we see that the probability $P(x, s)dx$ to be injected into the interval $[x, x + dx] \subset [-a, a]$ from the outside of $[-a, a]$ at time s, $s \geq 0$, is given by

$$P(x, s) = P_1(x, s) + P_2(x, s)\,,$$

where

$$P_1(x, s) = G(s)h_1(x)\,,$$

and

$$P_2(x, s) = G(s - 1)h_2(x)\,,$$

with

$$h_2(x) = \chi(\{x : x \in f_\epsilon([-a', -a])\})\frac{h_L}{|(\partial_x f_\epsilon)(f_\epsilon^{-1}(x))|}\,.$$

If we use the asymptotic behavior of G, as described in (3.5), then we see that for large fixed s the reinjection density is proportional to $h_1(x) + (1 - p)^{-1}h_2(x)$. Therefore, to some approximation, the same distribution can be expected for the injection density integrated over arbitrary return times. This density is compared with an experimental run in Fig. 4.
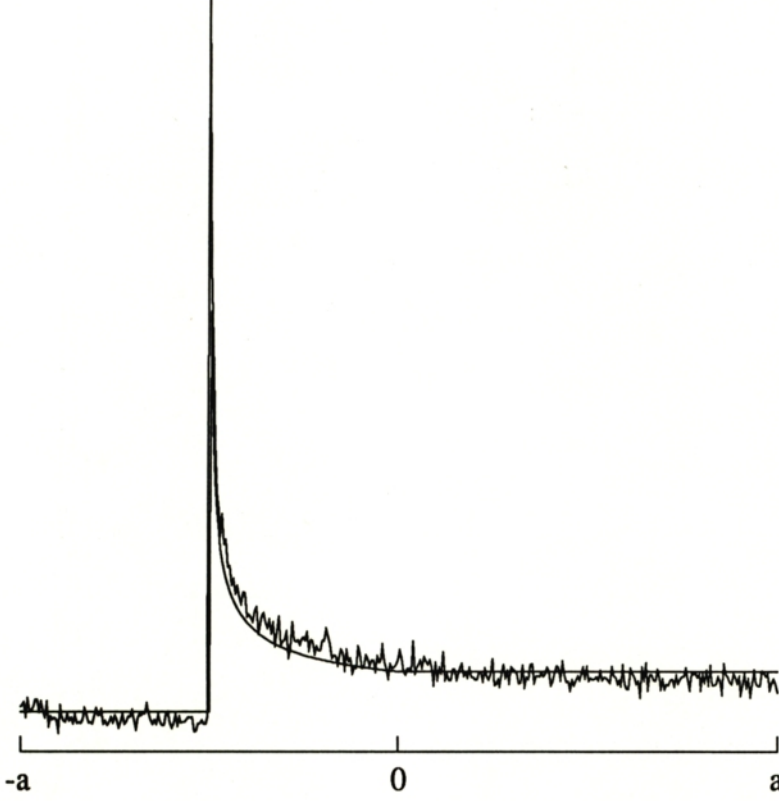
---

* The error is about 30%.

Fig. 4: The reinjection density into $[-a, a]$ for $\epsilon = 0.0003$. There were $3 \cdot 10^6$ iterations, leading to 39469 returns. The highest point represents 892 returns. Superposed is the theoretical curve.

From the laminar nature of the motion it is now easy to compute a model function for $\Delta(t)$. Expressed in continuous variables, the time needed to get from $x \in [-a, a]$ to a is

$$t(x) = \frac{1}{(\epsilon\kappa)^{1/2}} \left(\arctan((\kappa/\epsilon)^{1/2}a) - \arctan((\kappa/\epsilon)^{1/2}x) \right) .$$

Thus, we find

$$\Delta(t) = \int_{-a}^{a} dx \, P(x, t - t(x))\chi(t > t(x)) .$$

To have a better computational handle, we proceed as follows. Denote by X_0, $X_1, \ldots$ the successive preimages of a in $[0, a]$, $X_j = f_0^{-j}(a)$. From Equation(3.2), we have $X_{j-1} = X_j + \kappa X_j^2$, and $X_0 = a$. A straightforward calculation shows that
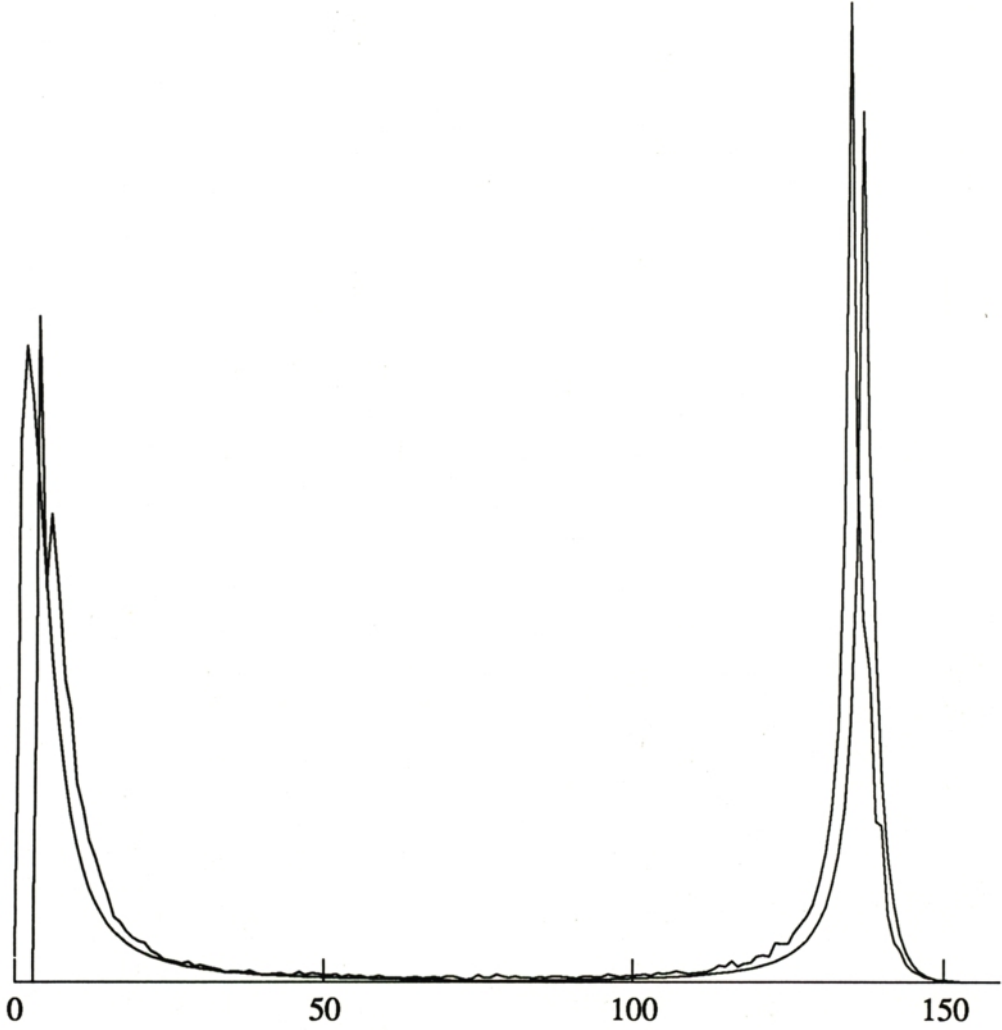
$$X_j \approx \frac{a}{a\kappa j + 1} ,$$

Fig. 5: The distribution $\Delta(m)$ as a function of m. The graph was obtained from $3 \cdot 10^6$ iterations of f_ϵ with $\epsilon = 0.0003$. We superpose the theoretical curve for $p = 0.385$, Eq.(3.9).

and

$$X_{j-1} - X_j = \kappa X_j^2 \approx \kappa \left(\frac{a}{a\kappa j + 1} \right)^2 .$$

The probability to find a return time of m after reinjection to the *right* of 0 is approximately equal to

$$\Delta_R(m) = \sum_{s=0}^{m-1} \text{Prob(injection time} = s) \times \text{Prob(injection into } [X_{m-s}, X_{m-s-1}]).$$

If we denote by n_{tot} the total time to move from $-a$ to a, then, for small ϵ, this leads

to

$$\Delta_R(m) \approx \sum_{s=\max(0,m-n_{\text{tot}}/2)}^{m-1} G(s)|X_{m-s} - X_{m-s-1}|h_1(X_{m-s})$$

$$\approx \sum_{s=\max(0,m-n_{\text{tot}}/2)}^{m-1} G(s)\frac{\kappa a^2}{(a\kappa(m-s)+1)^2} h_1\Big(\frac{a}{a\kappa(m-s)+1}\Big)$$

$$\approx \int_{\max(0,m-n_{\text{tot}}/2)}^{m} ds\, G(s)\frac{\kappa a^2}{(a\kappa(m-s)+1)^2} h_1\Big(\frac{a}{a\kappa(m-s)+1}\Big) .$$

The situation on the l.h.s. of 0 is similar. By Equation(3.3), we have

$$n_{\text{tot}} = 2\frac{1}{(\epsilon\kappa)^{1/2}} \arctan(a(\kappa/\epsilon)^{1/2}) \approx \frac{\pi}{(\epsilon\kappa)^{1/2}} .$$

We define $Y_{n_{\text{tot}}} = -a$, and $Y_{n_{\text{tot}}-j} = f_0^j(-a)$. For small ϵ, and $n_{\text{tot}}/2 \leq k \leq n_{\text{tot}}$, the Y_k are approximations to $f_\epsilon^{-k}(a)$ and we have, for k sufficiently near to n_{tot},

$$Y_k \approx \frac{-a}{a\kappa(n_{\text{tot}} - k) + 1}$$

$$Y_{k-1} - Y_k \approx \kappa \left(\frac{a}{a\kappa(n_{\text{tot}} - k) + 1}\right)^2 .$$

A point in the interval $[f_\epsilon^{-k}(a), f_\epsilon^{-k+1}(a))$ –where the preimages are taken in [-a,a]–will cross a after k steps. It follows that

$$\Delta_L(m) \approx \sum_{s=\max(0,m-n_{\text{tot}})}^{m-n_{\text{tot}}/2-1} G(s)|Y_{m-s} - Y_{m-s-1}|h_3(Y_{m-s})$$

$$\approx \sum_{s=\max(0,m-n_{\text{tot}})}^{m-n_{\text{tot}}/2-1} G(s)\frac{\kappa a^2}{(a\kappa(n_{\text{tot}} - m + s) + 1)^2} h_3\Big(\frac{-a}{a\kappa(n_{\text{tot}} - m + s) + 1}\Big)$$

$$\approx \int_{\max(0,m-n_{\text{tot}})}^{m-n_{\text{tot}}/2} ds\, G(s)\frac{\kappa a^2}{(a\kappa(n_{\text{tot}} - m + s) + 1)^2} h_3\Big(\frac{-a}{a\kappa(n_{\text{tot}} - m + s) + 1}\Big),$$

where $h_3 = h_1 + (1 - p)^{-1}h_2$. Finally,

$$\Delta(m) = \Delta_R(m) + \Delta_L(m) . \tag{3.8}$$

Replacing $h_3(x)$ by $h_1(x)$ and $G(s)$ by the approximation $G(s) = p(1-p)^s$ for $s \geq 0$ (although this is not such a good approximation for small s), we find a function

$$
\begin{aligned}
\Delta_{\text{th}}(m) = \text{const.}\Big(& \sum_{s=\max(0,m-n_{\text{tot}}/2)}^{m-1} p(1-p)^s \frac{\kappa a^2}{(a\kappa(m-s)+1)^2} h_R \\
& + \sum_{s=\max(0,m-n_{\text{tot}})}^{m-n_{\text{tot}}/2-1} p(1-p)^s \frac{\kappa a^2}{(a\kappa(n_{\text{tot}}-m+s)+1)^2} h_L \Big) \, .
\end{aligned}
\tag{3.9}
$$

We compare this function with an experimental run in Fig. 5 (the translation of the peaks is caused by the approximation for G).

In Fig. 6 below, we fix $\epsilon = 0.012$ and we compare the resonances for f_ϵ with the prediction of the theory we have developed. In order to obtain the resonances, we compute the correlation function from 180000 iterates of f_ϵ and we proceed in the same way as Isola [4] to find the poles of this experimental correlation function, using the method of interpolating exponentials [2]: We sample the correlation function at points C_k, $k = 0, \ldots, 40$. and write the (20,20) Padé approximant

$$
\sum_{k=0}^{40} C_k z^k = C_0 + \frac{Q_1(z)}{Q_2(z)} + \mathcal{O}(z^{41}) \, ,
$$

where Q_1 and Q_2 are polynomials of degree 20. (We normalize $Q_1(0) = 0$, $Q_2(0) = 1$.) We then find the complex roots of $Q_2(z) = 0$, using a program of Hoffmann [3], and we compute the residues of the poles of Q_1/Q_2. These are shown in Fig. 6 as discs centered at the poles, with area equal to the modulus of the residue and a line segment showing its phase. (This is done because two closeby residues with opposite phase could "cancel".) It is reassuring that whenever there are poles on the "wrong" side of the real axis then they have very small residues (remember that we only consider C_k with $k \geq 0$). We next consider the experimental distribution D, which approximates Δ, and find that $D(k) = 0$ for $k > 43$. We use Hoffmann's program to compute the roots ω of

$$
\sum_{k=0}^{43} D(k) e^{i\omega k} = 1.
\tag{3.10}
$$

By the same method we find the poles for the theoretical distribution Δ_{th} of Eq.(3.9). The determination of roots becomes somewhat unreliable when there are too many. Therefore, in Fig. 6 we have chosen ϵ relatively large. On the other hand, the asymptotics of (3.9) is better for smaller ϵ.
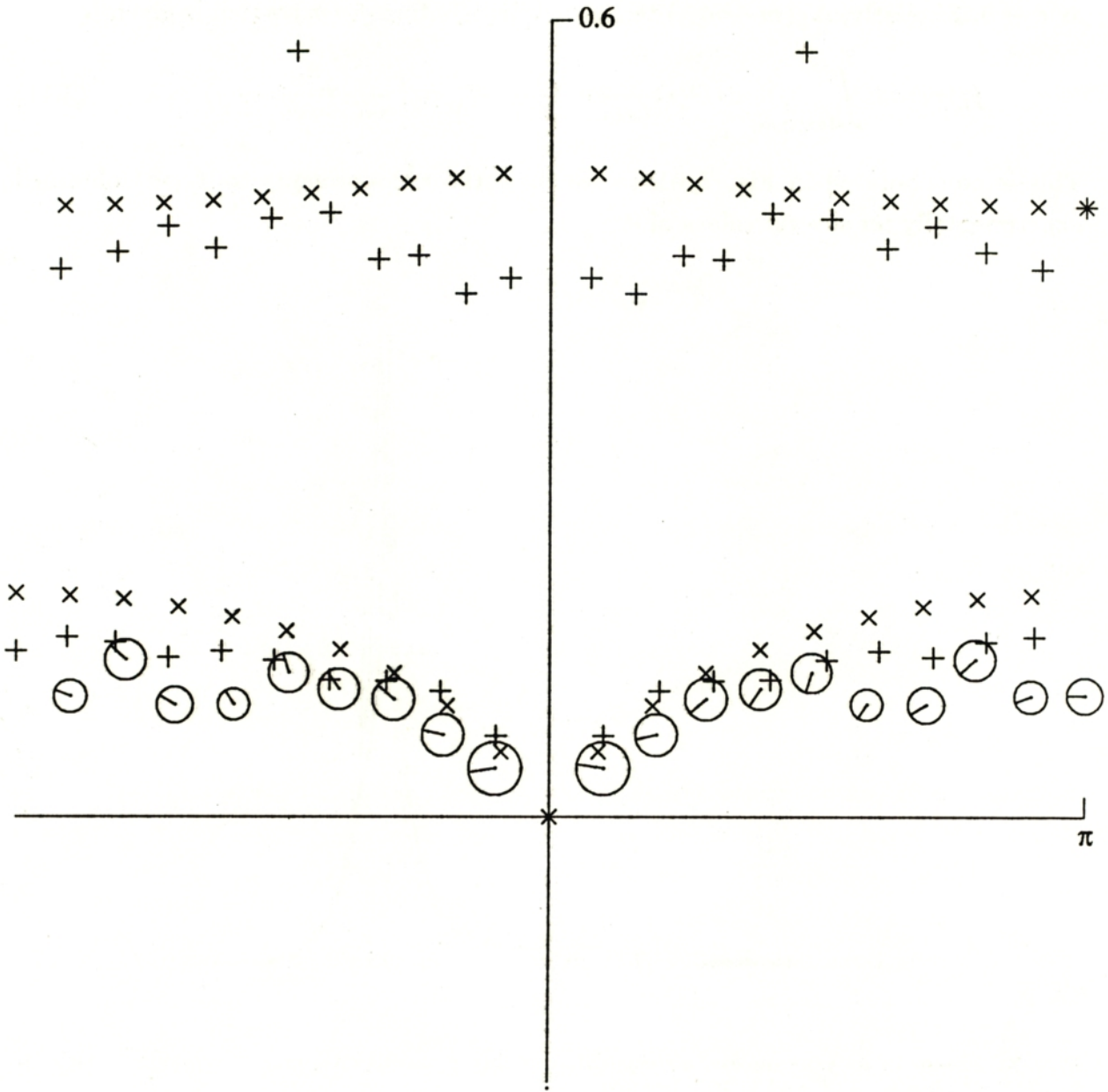
Fig. 6: The discs are centered at the poles of the correlation function for f_ϵ with $\epsilon = 0.012$, with area and angle representing the residue (cf. text). The $\times$ correspond to the prediction obtained through Lemma 2.1 and (3.9) for Δ_{th} and the $+$ are the roots of (3.10) for the experimental D.

It is tempting to perform an asymptotic analysis in powers of ϵ similar to that of (2.5). Unfortunately, this analysis does not lead to simple expressions in terms of the bifurcation parameter and of k, and hence we only sketch some of the essential steps in such a calculation. It is easy to see that $\Delta_R(m)$ tends to a limiting distribution $f_R(m)$

as $\epsilon \to 0$. Similarly, $\Delta_L(m + n_{tot})$ tends to a distribution $f_L(m)$ which is given by

$$f_L(m) \approx \int_{\max(0,m)}^{\infty} ds\, G(s) \frac{\kappa a^2}{(a\kappa(s-m)+1)^2} h_3\left(\frac{-a}{a\kappa(s-m)+1}\right). \qquad (3.11)$$

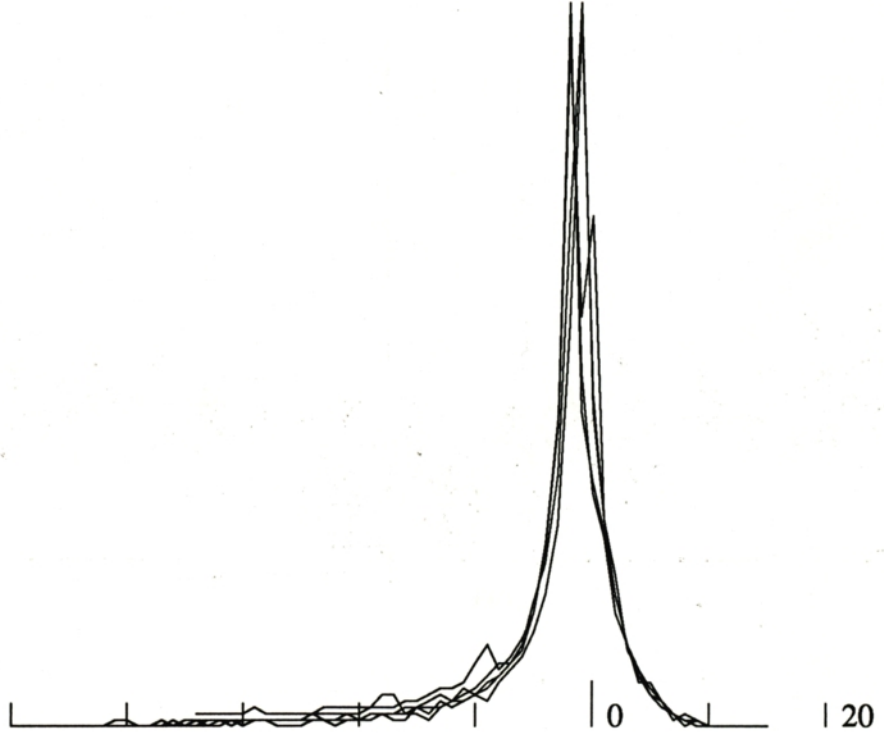This is corroborated in Fig. 7 where we show the approximants to $f_L(m)$ obtained experimentally for several values of ϵ.

Fig. 7: Shown is an experimental superposition of $\Delta(t + n_{tot})$ (with $n_{tot} = \pi/(\epsilon\kappa)^{1/2}$, for $\epsilon = 2 \cdot 10^{-6} \cdot 5^k$, $k = 0, \ldots, 4$, and $5 \cdot 10^6$ iterations.

However, the decay of f_L for negative m is quadratic and is seen to be a direct consequence of the spacing of orbit points near $x = 0$. Consequently, f_L and similarly f_R have moments which *diverge* as $\epsilon \to 0$. A perturbative analysis which we sketch in the Appendix shows that

Lemma 3.1. *For small ϵ the mean of f_L scales like $\log(\epsilon)$ and the moments of order $p \geq 2$ scale like $\epsilon^{-(p-1)/2}$.*

Given this information, we can now perform an analysis which is similar to the study of the Gaussian distribution in Section 2. By Lemma 3.1, the Fourier transforms of Δ_R and Δ_L have asymptotic expansions of the form

$$\hat{\Delta}_R(\omega) = a_R + \mathcal{O}(log\epsilon)\omega + \mathcal{O}(\epsilon^{-1/2})\omega^2\big(1 + \mathcal{O}(\omega)\big) \ ,$$

and

$$\hat{\Delta}_L(\omega) = e^{-i\omega n_{tot}}\Big(a_L + \mathcal{O}(log\epsilon)\omega + \mathcal{O}(\epsilon^{-1/2})\omega^2\big(1 + \mathcal{O}(\omega)\big)\Big) \ ,$$

from which one can deduce an expansion for the poles

$$\omega_k = \frac{2\pi k}{n_{tot}} + i\epsilon F(k,\epsilon) \ ,$$

for $k = 0, \pm 1, \ldots$. However, the function $F(k,\epsilon)$ has no simple expansion in terms of k and ϵ and depends on the details of Δ_R and Δ_L.

4. An Example with Period Three

We present here a few diagrams showing the situation which occurs after a period 3 saddle-node bifurcation and which illustrate the presence of *two* basic frequencies mentioned in Section 1. The example is taken to be the one-parameter family of maps $\mu \to f_\mu$, where $f_\mu(x) = 1 - \mu x^2$. For $\mu \in [0,2]$, the function f_μ maps the interval $[-1,1]$ to itself, and it is easy to check that for $\mu = \mu_0 = 1.75$, this map has a periodic point x_0 of period 3, and $\partial_x f_{\mu_0}^3(x_0) = 1$. As μ is *lowered* from this value, the period three disappears and intermittency is observed in much the same way as in the example of Section 3.

The correlation function has now *two* basic frequencies. One comes from the period three itself, and is already present for parameter values when the period is stable. In fact, in that case the orbit visits asymptotically three points y_1, y_2, y_3 in periodic order, and the correlation function equals

$$C_{0+3k} = \frac{y_1^2 + y_2^2 + y_3^2}{3} \ ,$$

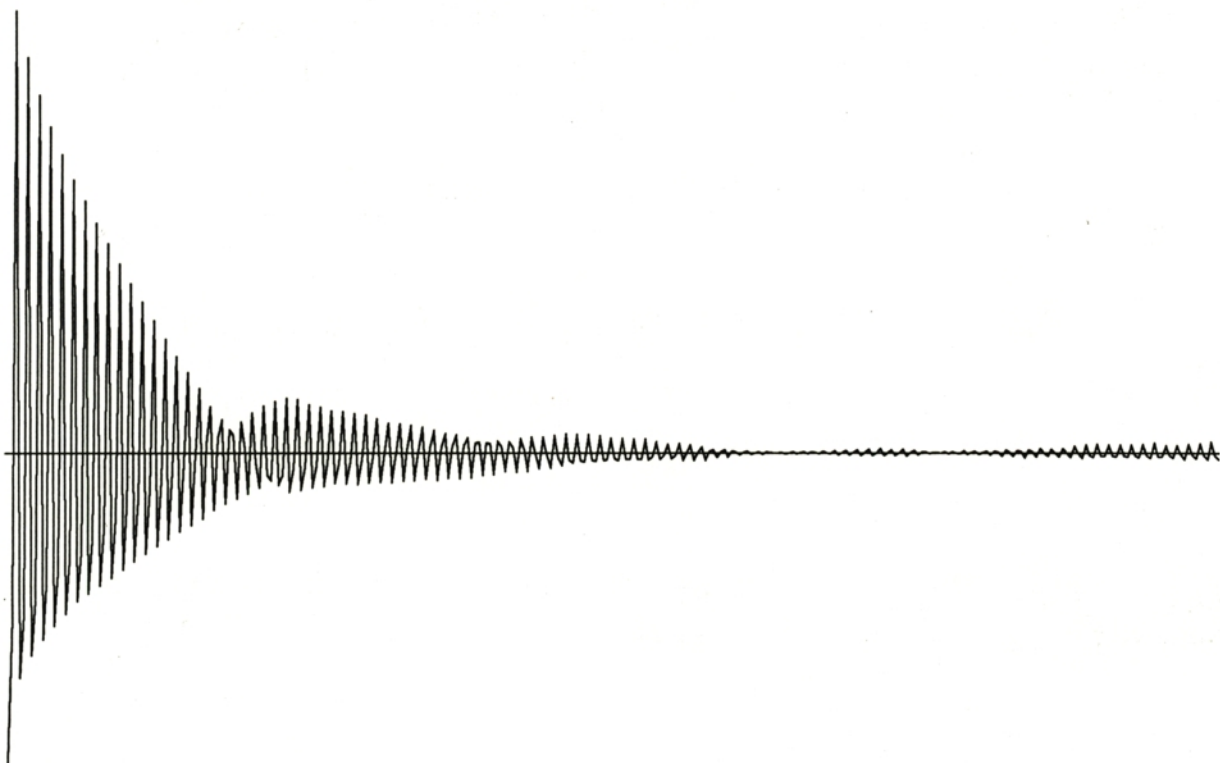$$C_{1+3k} = C_{2+3k} = \frac{y_1 y_2 + y_2 y_3 + y_3 y_1}{3} \ ,$$

Fig. 8: The first 320 values of the correlation function for $\mu = 1.75 - 0.0003$. Note the two basic periods.

for all k, and this is in general a periodic function of period 3. The other period is the *mean return time*, as in the example of Section 3. This leads then to a correlation function which is typically of the form shown in Fig. 8.

One can repeat the experiments from Section 3 and one is led to the same conclusions, replacing on occasion the function f_μ by the third iterate f_μ^3.

For example, we define the intervals I_n as follows: Denote by x_0 the fixed point of $f_{\mu_0}^3$ which is closest to the origin. We have $f_{\mu_0}^3(x_0) = x_0$ and $\partial_x f_{\mu_0}^3(x_0) = 1$, and numerical estimates show $x_0 \approx 0.032$. We say that I_n ends if the orbit "crosses" a point to the right of x_0, e.g. $x_1 = 0.05$ from left to right, more precisely, if, for some k, $f_\mu^k(x) \in [x_0, x_1]$ and $f_\mu^{k+3}(x) > x_1$. The interval I_{n+1} starts one time step after I_n ends. The results of a corresponding experiment are shown in Fig. 9.
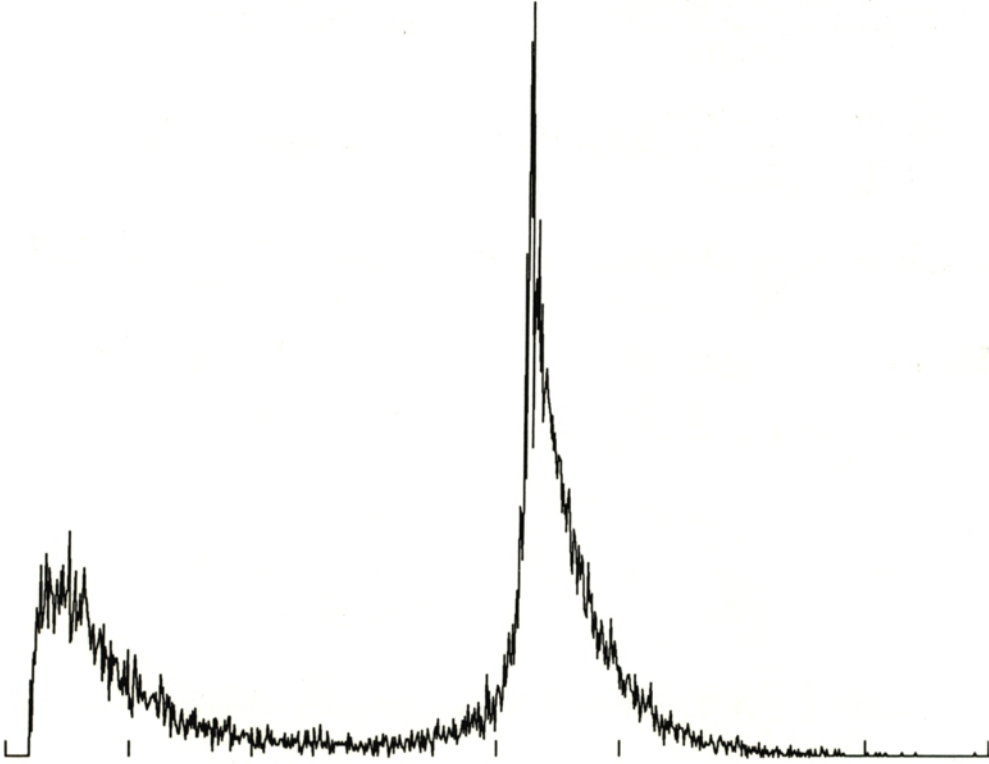
Fig. 9: The distribution $\Delta(m)$ as a function of m for $m = 0, \ldots, 900$. The graph was obtained from $5 \cdot 10^6$ iterations of f_μ with $\mu = 1.75 - 1 \cdot 10^{-5}$. The maximal height is 269, the exit point x_1 from laminarity is at 0.05.

Appendix. The Moments of Δ

We sketch the main steps in establishing the behavior of Δ_L and Δ_R as $\epsilon \to 0$. We fix our attention on Δ_L only, the case of Δ_R being slightly easier. For $m > n_{\text{tot}}$, the function $\Delta_L(m)$ is easily seen to have an exponential tail, and therefore the contributions to the moments coming from the region of integration $m > n_{\text{tot}}$ stay finite as $\epsilon \to 0$. Since the contributions from $m < n_{\text{tot}}$ will be seen to diverge as $\epsilon \to 0$ it will suffice to consider only those contributions. By (3.11), we find that for $n_{\text{tot}}/2 < x < n_{\text{tot}}$,

$$\Delta_L(x) \approx f(x) \equiv \int_0^{x-N/2} ds \, e^{-\alpha s} \frac{1}{(N - x + s + 1)^2} \, ,$$

where $N = n_{\text{tot}}$, $\alpha = -\log(1 - p)$, and where, for simplicity, we have set $a = 1$ and $\kappa = 1$. By definition, the function f has support in $N/2 < x < N$. We claim that

$$(A) \qquad \int_{N/2+1}^N dx \, f(x) = \text{const.} \, (1 + o(N))$$

(B) $\qquad$ $\dfrac{\int_{N/2+1}^{N} dx\,(N-x)f(x)}{\int_{N/2+1}^{N} dx\,f(x)} = \text{const. } \log(N)(1+o(N))$

(C) $\qquad$ $\dfrac{\int_{N/2+1}^{N} dx\,(N-x)^p f(x)}{\int_{N/2+1}^{N} dx\,f(x)} = \text{const. } N^{p-1}(1+o(N))\,,p=2,3,\ldots\,.$

From this, and the exponential decay of Δ_L for $m > n_{\text{tot}}$, Lemma 3.1 follows readily.

Proof. Equations (A)–(C) are obtained more easily by looking at the function

$$
\begin{aligned}
h(y) &= e^{-\alpha} f(-y+N) \\
&= e^{-\alpha} \int_0^{N/2-y} ds\, e^{-\alpha s}(y+s+1)^{-2} \\
&= \int_1^{N/2-y+1} ds\, e^{-\alpha s}(y+s)^{-2}\,,
\end{aligned}
$$

with support in $0 \le y \le N/2$. Note that we can exchange integrals,

$$
\int_0^{N/2} dy \int_1^{N/2-y+1} ds = \int_1^{N/2+1} ds \int_0^{N/2-s+1} dy\,.
$$

The expressions (A)–(C) lead to analogous integrals over h and we are led to estimate

$$
\int_1^{N/2+1} ds\, e^{-\alpha s} \int_0^{N/2-s+1} dy\, y^p(y+s)^{-2}\,.
$$

for $p = 0,1,2,\ldots$. E.g., for $p=1$, this integral equals

$$
\begin{aligned}
&\int_1^{N/2+1} ds\, e^{-\alpha s} \int_0^{N/2-s+1} dy\, \frac{(y+s)-s}{(y+s)^2} \\
&= \int_1^{N/2+1} ds\, e^{-\alpha s} \left[\log\left(\frac{N/2+1}{s}\right) - 1 + \frac{s}{(N/2+1)}\right]\,,
\end{aligned}
$$

which shows that the leading contribution is const. $\log(N)$, and this is (B). The other cases are handled similarly.

REFERENCES

[1] J.-P. Eckmann, L. Thomas and P. Wittwer: Intermittency in the presence of noise. J. Phys. A **14**, 3135–3168 (1981).

[2] P. Henrici: *"Applied and Computational Complex Analysis"*, New York, John Wiley (1977).

[3] Ch. Hoffmann: Weyl-Newton, ein globales Verfahren zur Bestimmung von Polynomnullstellen mit Fehlerschranken. Ph. D. thesis 5796, ETHZ (1976), Zürich.

[4] S. Isola: Resonances in chaotic dynamics. Commun. Math. Phys. (in print).

[5] E.N. Lorenz: Deterministic nonperiodic flow. Jour. Atmospheric Sc. **20**, 130–141 (1963).

[6] H. Mori, K. Shobu, B.C. So, and H. Okamoto: Spectral structure and universality of intermittent chaos. Physica Scripta **T9**, 27–34 (1985).

[7] H. Mori, H. Okamoto, B.C. So, and S. Kuroki: Global spectral structures of intermittent chaos. Prog. Theor. Phys. **76**, 784–801 (1986).

[8] M. Pollicott: On the rate of mixing of Axiom A flows. Invent. Math. **81**, 413–426 (1985).

[9] Y. Pomeau and P. Manneville: Intermittent transition to turbulence in dissipative dynamical systems. Commun. Math. Phys. **74**, 189–197 (1980).

[10] D. Ruelle: Flots qui ne mélangent pas exponentiellement. C. R. Acad. Sc. Paris **296**, Sér I, 191–193 (1983).

[11] D. Ruelle: One-dimensional Gibbs states and Axiom A diffeomorphisms. J. Differential geometry **25**, 117–137 (1987).

[12] D. Ruelle: Resonances for Axiom A flows. J. Differential geometry **25**, 99–116 (1987).